CrossMark

ORIGINAL RESEARCH PAPER

The role of the urban system dysfunction
in the assessment of seismic risk in the Mt. Etna area
(Italy)

F. Meroni[1] · G. Zonno[1] · R. Azzaro[4] · S. D'Amico[4] ·
T. Tuvè[4] · C. S. Oliveira[2] · M. A. Ferreira[2] · F. Mota de Sá[2] ·
C. Brambilla[3] · R. Rotondi[3] · E. Varini[3]

Abstract A procedure for seismic risk assessment is applied to the Mt. Etna area (eastern Sicily, Italy) through assessment of urban system dysfunction following the occurrence of an earthquake. The tool used is based on the Disruption Index as a concept implemented in Simulator QuakeIST, which defines urban disruption following a natural disaster. The first element of the procedure is the definition of the seismic input, which is based on information about historical seismicity and seismogenic faults. The second element is computation of seismic impact on the building stock and infrastructure in the area considered. Information on urban-scale vulnerability was collected and a geographic information system was used to organise the data relating to buildings and network systems (e.g., building stock, schools, strategic structures, lifelines). The central idea underlying the definition of the Disruption Index is identification and evaluation of the impact on a target community through the physical elements that most contribute to severe disruption. The procedure applied in this study (i.e., software and data) constitutes a very useful operational tool to drive the development of strategies to minimise risks from earthquakes.

Keywords Seismic impact · Disruption Index · Urban system · Risk measures · Mt. Etna area (Italy)

✉ F. Meroni
fabrizio.meroni@ingv.it

[1]   Istituto Nazionale di Geofisica e Vulcanologia, Milano, Italy

[2]   Instituto Superior Técnico, University of Lisbon, Lisbon, Portugal

[3]   Istituto di Matematica Applicata e Tecnologie Informatiche, Consiglio Nazionale delle Ricerche, Milano, Italy

[4]   Istituto Nazionale di Geofisica e Vulcanologia, Catania, Italy

🙋 Springer

1 Introduction

Mitigation is a key element of policies for disaster risk reduction. Through the implementation of disaster mitigation strategies, disaster risk-reduction benefits can be achieved, to the advantage of individuals, communities and infrastructure. In the project 'Urban Disasters Prevention Strategies using Macroseismic Faults' co-financed by the EU—Civil Protection Financial Instrument, DG ECHO Unit A5 (UPStrat-MAFA project 2012–2013), a tool that is specially adapted to identify prevention priorities was developed through an iterative procedure. This procedure allowed the analysis and optimisation of specific strategies to mitigate seismic risk, which were based on the quantification of costs and benefits of possible future interventions (e.g., for building stock, non-structural components, critical assets, critical infrastructure, lifelines, and so on).

The information on vulnerability is an element that together with ground-motion parameters can be used for the identification of risk. Some studies on measures of vulnerability have already been reported, like use of simulators, and vulnerability assessment of buildings, non-structural components, critical assets, lifeline (critical) infrastructures, and others. The new concept of global disruption (Ferreira 2012) has been introduced, with the objective being to provide a systematic way to measure earthquake impact in urban areas.

Earthquake scenario simulators developed to date show direct physical damage in terms of victims, buildings, essential facilities, and transportation systems, without including estimations of indirect losses or propagated effects (i.e., functional interdependencies) (Oliveira et al. 2014). As disruption to the systems and networks increases, the 'urban performance' decreases, which means that something dynamic has been replaced by something that has become static. In this context, we applied the Disruption Index (DI) to quantify the state of disorder that is induced by disruption of the urban structures and their functions. In other words, the DI provides a global measure of the effects of an earthquake that takes into account the impact on the local network of lifelines and infrastructure, and their interconnections. A framework is provided where urbanised areas are seen as a complex network where nodes have the role of sources that interact together in an interdependent fashion. Here, each player (e.g., urban function or physical asset) has its unique dependencies and interaction behaviours. Those properties are then used to identify which nodes are likely to introduce major disruption into the whole urban system, and also which nodes suggest greater risk reduction if an intervention takes place.

In this study, we present the application of this entire procedure to Mt. Etna, which is the largest active volcano in Europe and is well known for its continuous and intense eruptive phenomena. The assessment of risk at Etna is indeed a multidisciplinary matter (Fig. 1): the frequent summit activity with vigorous ash emissions causes problems for aeronautic traffic of the central Mediterranean Sea (Scollo et al. 2009, 2013); flank eruptions generate lava-flows that can destroy man-made features and invade cultivated and inhabited zones (Behncke et al. 2005; Del Negro et al. 2013); recurrent volcano-tectonic earthquakes damage buildings and infrastructure in the densely urbanised areas on the volcano slopes, which are also exposed to the impact of the less frequent, but large, regional earthquakes (Azzaro et al. 2013a).

Unfortunately, under some circumstances, these different typologies of threatening events can occur at the same time, as during the 2001 and 2002 Mt. Etna eruptions, just to mention the most recent cases (Branca et al. 2003; Alparone et al. 2004). The opportunities that the Mt. Etna volcano offers for testing methodological approaches in different application fields derive from its high degree of instrumental monitoring, together with the availability of the long record of historical information on seismic and volcanic

Fig. 1 Conceptual scheme of the main four typologies of risk that affect the Mt. Etna area. At present, these are dealt with separately (see text), but effective territory management should consider their integrated assessment
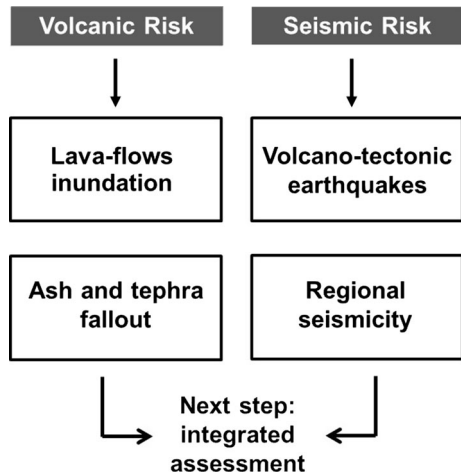

phenomena, features that are not common for other volcanic areas worldwide. In recent years, these have led studies to be undertaken that have been aimed at assessment of the seismic hazard at a local scale, due to the availability of both a detailed volcano-tectonic earthquake catalogue and a well-known seismotectonic model of the area.

To obtain the DI, we first estimate the seismic input; i.e., the scenario earthquake expressed in terms of the macroseismic intensity, using the procedure implemented for Mt. Etna in the PROSCEN software (Azzaro et al. 2013b). Taking in consideration the seismic risk only, we estimate the damage expected at the urban scale through the vulnerability of the different elements organised in a geographic information system (GIS) format. The main fields of information here include building typologies, locations of schools and other strategic infrastructure, type and patterns of essential lifelines, and others. Finally, we identify the municipalities that are more exposed to a given scenario earthquake, to show the results and limits of the application that can be overcome in future investigations.

2 Impact of tectonic earthquakes on seismic risk assessment in the Mt. Etna area

The Mt. Etna area is exposed to the damaging effects of both regional earthquakes and local volcano-tectonic events (Azzaro 2004). These earthquakes include large crustal events ($6.4 \leq M_W \leq 7.4$), such as the 1169 and 1693 earthquakes in southeastern Sicily, the 1818 earthquake near Catania, and the 1908 earthquake in the Messina Straits (Rovida et al. 2011), just to mention the main events (Fig. 2a). These shocks produced severe damage and even devastation in the Catania area and in the territories nearby, including the eastern sector of Mt. Etna, and they thus define the high level of seismic hazard along the whole eastern sector of Sicily (estimated at 50 years; see MPS Working Group 2004).

However, as indicated, the Mt. Etna area is also under the effects of local volcano-tectonic earthquakes that, albeit of low magnitude ($M_L \leq 5.1$; according to Azzaro et al. 2011), can produce severe macroseismic effects in areas of limited extent. The maximum intensities (I_{max}) here can reach up to X on the European Macroseismic Scale (EMS; see Grünthal 1998) because of the shallowness of the foci ($H \leq 5$ km; see Sicali et al. 2014). The stronger earthquakes can also be accompanied by extensive surface faulting, with end-to-end rupture lengths of up to 6.5 km, and vertical offsets of up to 90 cm, as active
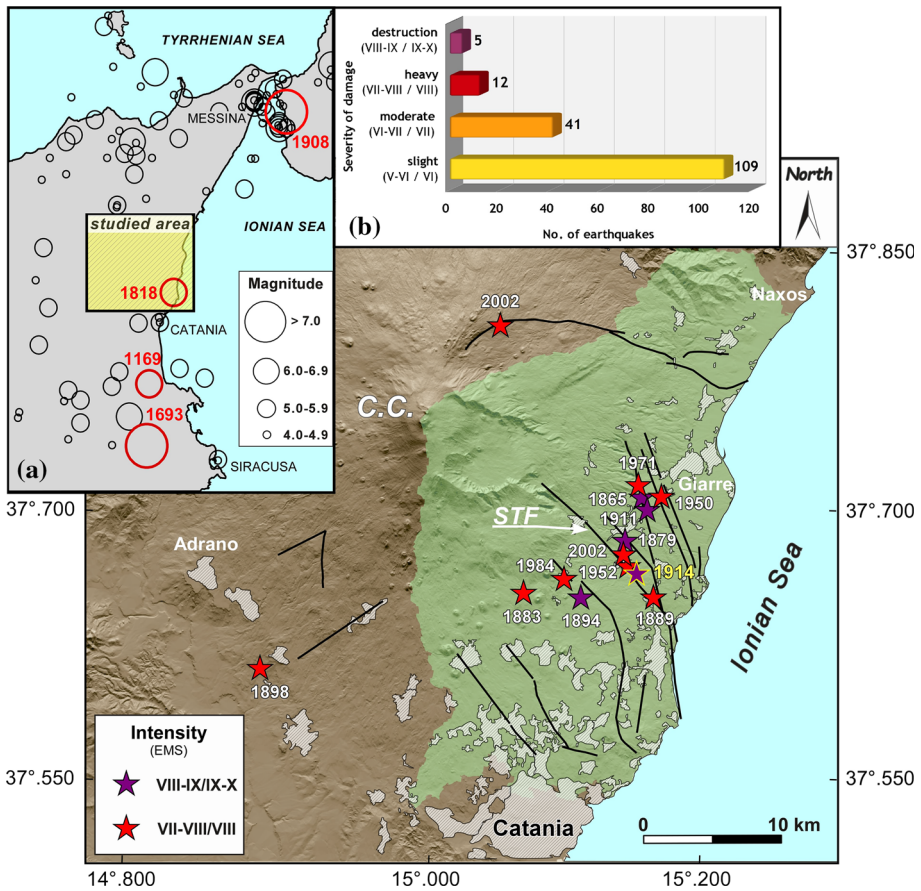
Fig. 2 Distribution of the volcano-tectonic earthquakes with epicentral intensity $I_0 \geq$ VII–VIII that occurred from 1832 to 2013 (CMTE Working Group 2014). *Green* the study area; *grey* the urbanised zones; *black solid lines* active faults; *STF* S. Tecla fault; *C.C.,* central craters. *Inset map* **a** regional seismicity from 1000 to 2006 (Rovida et al. 2011), where the *dates* indicate the largest regional events that influenced the seismic hazard in the Mt. Etna region. *Inset* **b** frequency of damaging earthquakes according to the severity of their effects

tectonic evidence that is indicative for the recognition of the causative faults (Azzaro 2004). Furthermore, the very high occurrence of these events represents a significant source of hazard at the local scale; indeed, over the last 180 years the catalogue of Etnean earthquakes (Catalogo Macrosismico dei Terremoti Etnei—CMTE) reports that there were 167 shocks that exceeded the damage threshold, with some 15 having produced heavy damage or destruction (CMTE Working Group 2014) (Fig. 2b). It is of note that most of these earthquakes, and mainly the largest ones, were located on the eastern flank of the Mt. Etna volcano, which is crossed by a dense network of highly active seismogenic faults (Fig. 2). The significance of these structures in terms of hazard is relevant, as they contribute to the same level of shaking that can be produced by the regional earthquakes, although with exposure times that are much shorter (10–30 years; see Azzaro et al. 2013a).

For the application of the DI to the Mt. Etna area, we therefore considered the lower eastern flank of the volcano, because of the high degree of risk that arises from the dense

urbanisation—28 municipalities in this area, with a total population of about 400,000 inhabitants—and the presence of relevant infrastructures and life-lines. As well as confirming and better detailing the seismic hazard of the eastern flank of Mt. Etna, this study carried out in the framework of the UPStrat-MAFA project and through disaggregation analysis (Azzaro et al. 2015) has shown that the S. Tecla Fault is the greatest contributing structure to the hazard at the level of Mt. Etna volcano. This result is indeed consistent with the earthquake rupture forecasts obtained by time-dependent approaches that have identified this fault as the most probable structure to be activated in the next 5 years (2013–2017; see Azzaro et al. 2013a).

For the seismic risk analysis presented in this study, we therefore selected the largest historical event known to have occurred in the Mt. Etna area; namely, the 1914 Linera earthquake (Azzaro et al. 2013b). This earthquake was well documented in several contemporary reports (main ones by Platania 1915; Sabatini 1913, 1915): the village of Linera and neighboring settlements were almost entirely destroyed, with a life toll of 70 victims; other localities, such as S. Venerina, Zafferana Etnea and a few others near Acireale suffered severe to heavy damage. The shock was felt throughout the Mt. Etna area. Ground ruptures opened in the epicentral area along the strike of the S. Tecla Fault, with a length of ca. 6 km, and the coseismic vertical offset was 50 cm. The source parameters of the 1914 earthquake used for the analyses hereinafter are from the 2011 version of the Parametric Catalogue of Italian Earthquakes (CPTI catalogue; Rovida et al. 2011): epicentre, latitude 37.659, longitude 15.149; epicentral intensity, I_0 IX–X; magnitude M_W 5.3.

3 The concept of the Disruption Index of a livelihood system

All communities are at risk and face potential disaster if they are not well prepared. When critical services and functions are disrupted for longer times than are reasonable, the consequences can be severe. The DI was designed to help to quantify the state of disorder induced by disruption of the urban structures and its systemic functions (Fig. 3) (Ferreira 2012; Oliveira et al. 2012; Ferreira et al. 2014).
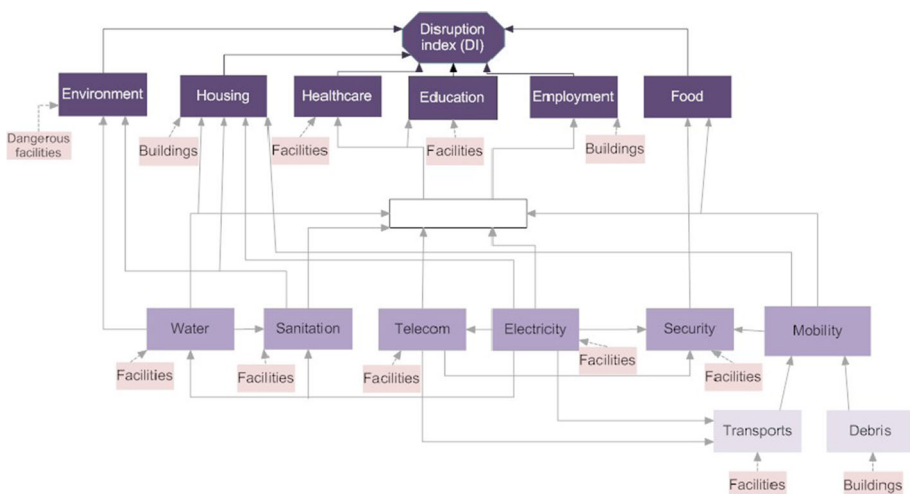
Fig. 3 Disruption Index: to quantify the state of disorder induced by disruption of the urban structure and its functions. This is based on the dimensions of human needs (along the top)

The purpose of the DI is to condense complex problems and multidimensional situations that involve earthquake impact on livelihood in a concise and easier way, without the need to assign a priori weights to the variables. This can provide institutions and communities with a process to identify elements at risk and ways to reduce this risk.

A complete description of this method and the particular variables and functions selected for the analysis can be found elsewhere (Ferreira et al. 2014). Moreover, Ferreira et al. (2015) carried out an analysis at the geographic scale, showing the results for a few cities as well as for the entire region of Algarve.

The physical damage to each part of the infrastructure is combined through a set of rules to determine the Disruption Index, with consideration of all of the interdependencies (Fig. 3). Briefly, the DI is derived from established and classified functions, using dimensions of human need, with the most fundamental being: environment, housing, healthcare, education, food, and employment. Each dimension contains the functions (i.e., service components) that have impact on welfare and urban life aspects, like water, sanitation, telecommunications, electricity, transportation network, and existence of debris. The propagation and cascading effects are calculated in a bottom-up sequence that starts with the physical damage that is directly suffered by the exposed assets, and proceeds to the impact that each physical element experiences via the functional performance of the services/components that depend on them. Finally, this reaches the top level of the DI.

At the end, each level of the DI conveys the relevant disruptions and influences (e.g., physical, functional, social, economic, environmental) that a given geographic area is subjected to when exposed to an adverse event (Table 1). Mapping the earthquake impact on the physical and social environment through the use of the DI provides an important tool to define realistic risk mitigation strategies. The dependency of the different levels of the DI on the levels of disruptions of the 6 dimensions of human needs is shown in Fig. 4 (for more details, see Ferreira et al. 2014).

The above concept describes the methodology that was experimented with for the Mt. Etna area, which required as the first step the preparation of several datasets, according to their availability.

4 Forecast of the seismic scenario: PROSCEN 0.9

On the basis of knowledge of the seismicity of a region (e.g., historical seismicity, location of faults, effects produced by past events), the evaluation of the impact of a future earthquake on an urban environment in a given area requires a quantitative picture of the possible effects of such an event on the components of the environment: the buildings, infrastructure and facilities. This information can be obtained by estimating the macroseismic effects generated by the earthquake. This provides the spatial distribution of the damages, which is expressed through the macroseismic intensity estimated at sites that surround the epicentre.

As the occurrence of seismic events of similar magnitude in different areas might produce quite different effects in terms of the level and extent of damage, the estimate should be the result of both global information of the phenomenon and the local characterisation: the former is drawn from an as-large-as possible learning set, the latter is obtained from past observations in the area under study. Moreover, the nature of the quantities involved requires the application of probability models and methods.

Table 1 Qualitative descriptors of the Disruption Index, with impact levels numbered in decreasing order of urban disruption/dysfunction

Impact level	Description of impact level
V	From serious disruption at physical and functional levels, to paralysis of the entire system: buildings, population, infrastructure, health, mobility, administrative and political structures, among others. Lack of conditions to carry out the functions and activities of daily life. High cost for recover
IV	Starts with paralysis of the main buildings and the housing, administrative and political systems. The region affected by the disaster has moderate damage and a large percentage of buildings totally collapsed, as well as victims and injuries and a considerable number of homeless, because their houses have been damaged, which, although not collapsed, is enough to lose their function for housing. Normal daily activities are disrupted; school activities are suspended; economic activities are at a stand-still
III	Part of the population might lose their property permanently and need permanent relocation, which means strong disturbance to everyday life. This level is determined by significant dysfunction in terms of equipment, critical infrastructure and loss of some assets and certain disorder involving the conduct of professional activities for some time. The most affected areas show significant problems in mobility due to the debris and damage to the road network. Starts with significant problems in providing food and water, which must be ensured by the Civil protection
II	The region affected by the disaster has some homeless (ca. 5 %) due to some damage to buildings, which affects the habitability of a given geographical area. Some people might experience problems of access to water, electricity and/or gas. Some cases require temporary relocation
I	The region affected by the disaster continues with the normal functions. There are no injured, killed or displaced people. Some light damage might occur (non-structural damage) that can be repaired in a short time, and sometimes there is temporary service interruption. The political process begins with an awareness that the problem exists, and some investment in strengthening policy and risk mitigation should be made

In our case, the learning set was the Italian DBMI11 database (Locati et al. 2011), which contains more than 86,000 data points related to 1681 earthquakes. To have a reliable database of the seismic decay in Italy, we considered the most informative macroseismic fields: 298 events of epicentral intensity MCS ≥ V, each with at least 40 data points. On the basis of this information, we can express a prior version of the probability model for the intensity at the site, and then we can fit this to the particular features of the attenuation observed on the eastern flank of Etna in a set of 57 fields (CMTE Working Group 2014).

A preliminary analysis of some of the macroseismic fields was performed through a non-parametric statistical tool, data depth functions (Agostinelli and Rotondi 2015); this analysis led up to assume a circular pattern when failing seismotectonic information, and an elliptical pattern when the length and strike of the fault rupture are evident from faulting phenomena described in the coeval chronicles or by analysing the distribution of the more relevant macroseismic effects.

The construction of the model consists of the following elements (Rotondi and Zonno 2004; Zonno et al. 2009): (1) The space surrounding the epicentre is divided by J adjacent concentric annuli of fixed width, with the assumption that at all of the sites in an annulus the intensity attenuates in the same way; (2) The intensity at site I_s, and correspondingly, the decay $\Delta I = I_0 - I_s$, are considered as binomial distributed random variables, according to Eq. (1):

	Environment	Housing	Food	Healthcare	Education	Employment	Mobility	Power supply	Telecom supply	Transportation	Debris	Water supply	Sanitation	Security	Dangerous facilities	Electrictic facilities & components	Transportation facilities & components	Water facilities & components	Sanitation facilities & components	Telecom facilities & components	Schools	Healthcare facilities	Security facilities & components	Building stock
DI																								
I		II																						
II	II			III	III	II																		
III		III	II	IV	IV	III																		
IV	III	IV				IV																		
V	IV	V	III																					
Environment																								
I																								
II									II			II		II										
III									III			III		III										
IV																								
Housing																								
I																								
II								II				II	II											II
III							III																	III
IV							IV	III				III	III											IV
V																								V
Food																								
I																								
II							III							III										
III							IV							IV										
Healthcare																								
I																								
II							II									II		II	II	II			II	
III							III									III		III	III	III			III	
IV							IV															IV		
Education																								
I																								
II								II				II	II								II			
III							II	III	III			III	III								III			
IV							III														IV			
Employment																								
I																								
II								II	II			II	II											III
III							III	III	III			III	III											IV
IV							IV																	V

Fig. 4 Impacts of the levels of disruptions of the fundamental areas of human needs and functions of the system on the different levels of DI (from Ferreira et al. 2014, 2015)

$$Pr(I_s = i \mid I_0 = i_0, p) = Pr(\Delta I = i_0 - i \mid I_0 = i_0, p) = \binom{i_0}{i} p^i (1-p)^{(i_0 - i)}, \qquad (1)$$

where according to a Bayesian approach, the parameter p is a beta distributed random variable:

$$Be(p; \alpha, \beta) = \frac{\Gamma(\alpha + \beta)}{\Gamma(\alpha)\Gamma(\beta)} \int_0^p x^{\alpha-1}(1-x)^{\beta-1} dx, \qquad (2)$$

with the α and β hyperparameters that include the prior information on the phenomenon; (3) The posterior beta distribution of the parameters p is computed on the basis of the current macroseismic fields, and p is estimated through its posterior mean.

Assigning the hyperparameters is one of the key points in Bayesian statistics. Considering that the probability of null decay in each j-th annulus is given by $Pr(\Delta I = 0 | I_0 = i_0, j) = p_j^{i_0}$, we can roughly estimate this probability by the relative frequency of the null decay $N_j(i_0)/N_j$, where $N_j(i_0)$ is the number of sites in the j-th annulus where the intensity at the site is not smaller than the epicentral intensity. $N_j(i_0)$ is obtained by analysis of the fields of the learning set, after clustering them into four classes that are homogeneous from the attenuation viewpoint, through a hierarchical agglomerative clustering method. This works on some statistical summaries of the sets of distances from the epicentre to the sites with the same decay ΔI (Zonno et al. 2009). Hence:

$$E_0(p_j) = \left(N_j(i_0)/N_j\right)^{1/i_0} = \alpha_{j,0}/\left(\alpha_{j,0} + \beta_{j,0}\right); \tag{3}$$

inverting this equation and that of the variance of p_j, we get the prior value of the hyperparameters in each annulus.

These values are then updated using the data contained into the macroseismic fields of Mt. Etna, so that the estimate of p_j, for each $j = 1, \ldots, J$, is given by its posterior mean:

$$\hat{p}_j = \frac{\alpha_{j,0} + \sum_{n_j=1}^{N_j} i_s^{(n_j)}}{\alpha_{j,0} + \beta_{j,0} + I_0 \cdot N_j}, \tag{4}$$

where $i_s^{(n_j)}$ is the intensity at the n_j-th site inside the jth annulus, and N_j is the total number of sites in that annulus. By smoothing the posterior mean of p in each annulus through an inverse power function $g(d) = (\gamma_1/d)^{\gamma_2}$, we can express this parameter as a continuous function of the epicentral distance d. In this way we can estimate I_s at any distance d from the epicentre by using what we call the smoothed binomial function:

$$\Pr_{smooth}(I_s = i | I_0 = i_0, d) = \binom{i_0}{i} g(d)^i (1 - g(d))^{(i_0 - i)}. \tag{5}$$

The mode of the smoothed binomial distribution, i_{smooth}, is taken as an estimate of the intensity at site I_s; moreover, through the posterior distribution of the parameters, the Bayesian paradigm also provides rational measures of the parameter uncertainties.

In Azzaro et al. (2013b), the anisotropic case was modelled by returning to the isotropic model through a plane transformation that converts the ellipse with the major axis equal to the fault rupture into the basic circle.

Hence, Eq. (5) allows us to simulate a damage scenario when an earthquake of fixed epicentral intensity may occur at a given location; in addition to the most probable scenario, we can compute the intensities at the site that are not exceeded with chosen probability thresholds; e.g., with 25 and 75 % probability (Rotondi et al. 2012). This is particularly important because the evaluation of the DI starting from scenarios of different probabilities provide a measure of the uncertainties of the effects produced by the selected earthquake that occurred on 8 May, 1914. The choice was motivated because this earthquake was not only the largest one (IX/X on the EMS scale), but also because it has a relatively rich macroseismic dataset (82 felt reports). Figure 5 shows the damage scenario of the earthquake in terms of the EMS intensity, as estimated by the software package PROSCEN (PRObabilistic damage SCENario; Rotondi and Zonno 2010; Azzaro et al.
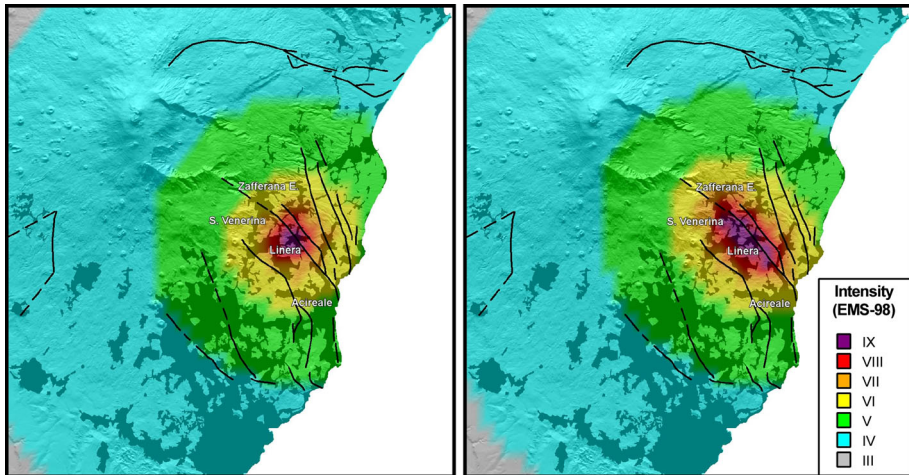
Fig. 5 Seismic scenarios, for the 1914 earthquake, with epicentral intensity $I_0 =$ IX–X EMS located on the eastern flank of Mt. Etna, along the S. Tecla Fault, simulated according to a point-source model (isotropic model; *left*) versus a linear finite fault (anisotropic model; *right*)

2013b). We can recall that PROSCEN simulates intensity shaking maps given the parameters of the location and the epicentral intensity of the earthquake (for theoretical details see Rotondi et al. 2015).

5 The QuakeIST simulator

QuakeIST$^{®}$ is an integrated earthquake scenario simulator that is based on GIS. It was developed by the Instituto Superior Técnico (IST) of the University of Lisbon (Portugal), to perform risk calculation and damage propagation using the DI (Ferreira et al. 2014). This opens up new territory for earthquake science and engineering, with the goal of reducing the potential for loss of life and property.

The architecture of QuakeIST$^{®}$ consists of four components: an urban geo-database; a model library; a simulation module; and the output. The urban geo-database provides basic spatial and statistical data used in the GIS platform for earthquake scenario simulation. The model library contains four sub-models (i.e., the ground motion, vulnerability, damage and DI models), which correspond to the key stages involved in the earthquake scenario simulations. The simulation module serves as an operation centre that integrates data and models. After the simulation is complete, statistical maps and tables constitute the resulting output. This QuakeIST$^{®}$ output helps to identify the most important factors and systems that contribute to the urban disruption, thereby contributing to the arranging of plans and guidance for short-term, medium-term, and long-term investment projects to reduce risk. A more detailed description of this integrated software can be found in Mota de Sá et al. (2015).

Up to now, QuakeIST$^{®}$ has been applied to Portugal, Iceland, Italy and Spain. Inside these countries, the test areas (i.e., the Algarve region in Portugal, Hverageroi in Iceland, Mt. Etna in Italy, Lorca in Spain) were chosen because they have the attributes of an urban area that represented an interdependent system that contained several interconnections for

Table 2 Elements at risk that were considered in the analysis

Residential buildings	Local transformers
Schools	Natural gas pressure reduction and measurement stations
Healthcare facilities	Natural gas pipes
Security facilities	Water pipes
Bridges	Wastewater pipes
Power stations	Explosives storage and inflammable liquid tanks

research on multiple infrastructure interdependencies. Overall, some of the elements at risk considered in these four urban areas, according to their availability, are given in Table 2.

The possible sources of the data for the elements at risk are the basic available data obtained with the support of the regional or national institutions, as the census data, and improved under the guidance of local experts.

Using the data available, inventories were drawn up for residential buildings, educational institutions, healthcare facilities and additional buildings, and classified into several groups that were qualified according to their structural characteristics. The lifeline inventory for each area was also compiled in a GIS environment, which consisted of digitised location and facility attributes.

Each type of structure and infrastructure has its own dynamic response characteristics, and hence a particular structural analysis is needed. To assess the consequences and impact of earthquake scenarios, we not only need tools to predict the physical consequences, but also to assess the vulnerability, and thus potential damage, to the surrounding environment, infrastructure and population. The literature review addressed the issue of the vulnerability, or fragility, of the relationships for each component subjected to ground shaking (Table 3). The parameter intensity in Table 3 is the intensity at the site that has been evaluated by the method implemented in the software package PROSCEN and is described in Sect. 4. Physical vulnerabilities are associated with buildings, infrastructure and lifelines. These vulnerabilities are agent-specific and site-specific. Furthermore, they also depend on the design, construction and maintenance specifics.

However for each of the elements at risk we have considered the set of available fragility functions already coded in the QuakeIST software (see Table 3). Many other relations could be considered and applied in this case study, in particular those more specifically developed for the Italian case. A typical example could be the relation adopted for storage and inflammable liquid tanks discussed in the paper by Grimaz (2014).

6 Vulnerability of buildings, urban infrastructure and systems

In this section the basic data are described that relate to the vulnerability of the buildings, and urban infrastructure and systems of the case-study area of Mt. Etna.

6.1 Residential buildings

To carry out vulnerability analysis on a regional scale, the size of the building stock can be inferred from data collected during the Italian census, as correctly adapted for the purpose of the vulnerability evaluation for the whole Italian territory (Meroni et al. 1999, 2000).

Table 3 The different seismic inputs for the different elements of risk in the urban system analysis

Element at risk	Methodology	Parameter	Comments
Buildings	Giovinazzi and Lagomarsino macroseismic method	Intensity EMS98	Distinction according to building typology
School buildings	Giovinazzi and Lagomarsino macroseismic method	Intensity EMS98	Distinction according to building typology
Healthcare buildings	Giovinazzi and Lagomarsino macroseismic method	Intensity EMS98	Distinction according to building typology
Security buildings	Giovinazzi and Lagomarsino macroseismic method	Intensity EMS98	Distinction according to building typology
Bridges	ERSTA project	Sa(T)	$P[dg \geq k] = N[Ln(PGA/mk)/bk]$
Power stations	Syner-G project	PGA	$P[dg \geq k] = N[Ln(PGA/mk)/bk]$
Local transformers	ERSTA project	PGA	$P[dg \geq k] = N[Ln(PGA/mk)/bk]$
Natural gas pressure reduction and measurement stations	Syner-G project	PGA	$P[dg \geq k] = 1/2\{1 + erf[Ln(PGA/mk)/bk\sqrt{2}]\}$
Natural gas pipes	Syner-G project	PGV	Repair rate: $RR[R/km] = ko \times k1 \times PGVk2$ [cm/s]
Water pipes	HAZUS mode	PGV	Repair rate: $RR[R/km] = ko \times k1 \times PGVk2$ [cm/s]
Wastewater pipes	HAZUS model	PGV	Repair rate: $RR[R/km] = ko \times k1 \times PGVk2$ [cm/s]
Explosives storage and inflammable liquid tanks	HAZUS model	PGA	$P[dg \geq k] = N[Ln(PGA/mk)/bk]$

Sa(T) spectral acceleration, *PGA* peak ground acceleration, *PGV* peak ground velocity

The census data are usually the primary source to assess residential building vulnerability over large areas, as they provide uniform cover of the whole country and make it possible to estimate the total number of buildings and their total volume. In the present study the size of the residential building stock was inferred from the 1991 Italian National Institute of Statistics (ISTAT) census (ISTAT 1991).

The data were grouped according to the census sections, and the vulnerability indices were evaluated using the approach proposed by Giovinazzi and Lagomarsino (2001), Lagomarsino and Giovinazzi (2006) and Bernardini et al. (2007). The ISTAT data on residential buildings also allows the definition of the frequencies of groups of homogenous structures, with respect to a number of typological parameters; i.e., vertical structures, age of construction, number of storeys, state of maintenance, and state of aggregation with adjacent buildings (see Table 4). Unfortunately, due to recent privacy regulations, the more recent ISTAT census data (i.e., the surveys of 2001 and 2011) provide values in an aggregated way only, which constrained the vulnerability evaluation to rough estimations. The availability of these data in an aggregated form only at the municipal level, without census section details and with few typological features on age, materials, building height, and other factors, has not recommended the use of such census data for vulnerability investigations (e.g., Crowley et al. 2009).

Table 4 Typological classes of building vulnerability identified in the ISTAT census data

Structural typology	Age	Number of floors	Structural context	Level of maintenance
Masonry	Pre-1919	1 or 2	Isolated	Good
Concrete—reinforced	1919–1945	3, 4 or 5	Block	Low
Concrete—soft floor reinforced	1946–1960	6 or more		
Other typologies	1961–1971			
	1972–1981			
	Post-1981			

Using the 1991 ISTAT data, and adopting the methodology proposed by Giovinazzi and Lagomarsino (2001) and Lagomarsino and Giovinazzi (2006), the data are grouped according to the census sections and their structural category. According to other typological classes derived from the ISTAT data (e.g., age, floors, structural context, maintenance), the starting vulnerability index of each category was modified through the so-called behaviour modifiers. The given score can cause an increase or decrease in the starting vulnerability index that will be proportional to the number of buildings identified by that behaviour modifier (D'Amico et al. 2015). The scores chosen in this study are consistent with data published in a study of vulnerability evaluation carried out over large areas in the Italian territory (Meroni et al. 1999, 2000). That study used the reference municipalities in which the Gruppo Nazionale per la Difesa dai Terremoti (GNDT; National Group for the Defence Against Earthquakes) vulnerability forms were available (levels I and II), and evaluated the average vulnerability index for homogeneous groups of buildings according to the different ISTAT census classes. For example, for each age group of masonry buildings, it was possible to evaluate the change in the vulnerability index according to the number of floors, the structural context, and the level of maintenance.

Following the above-described approach, the seismic vulnerability index, I_V, for each building typology was evaluated, which varies between 0 and 1, and is independent of the hazard severity level. Furthermore, an average seismic vulnerability of the region can be obtained by weighting the typology vulnerability index according to the several typologies in the area, thereby obtaining a synthetic vulnerability index to display and compare the vulnerability of the different census sections. More details on the vulnerability evaluation for residential buildings are given in (D'Amico et al. 2015).

6.2 Fragility curves for residential buildings

According to the Lagomarsino and Giovinazzi (2006) approach, they estimated an expected damage grade, μ_D, for a building typology according to the following equation:

$$\mu_D = 2.5 \cdot \left[1 + \tanh \left(\frac{I + 6.25 \cdot I_v - 13.1}{2.3} \right) \right], \tag{6}$$

where μ_D is the mean damage grade of D, the random variable for damage (grade 1, slight; grade 2, moderate; grade 3, heavy; grade 4, very heavy; grade 5, collapse), I is the

intensity, and I_V is the vulnerability index. The fragility curves for $P(D > d \mid I)$ are modelled according to a beta distribution, with a probability density function given by:

$$p_\beta(d) = \frac{\Gamma(q)}{\Gamma(p) \cdot \Gamma(q-p)} \cdot \frac{(d-a)^{p-1} \cdot (b-d)^{q-p-1}}{(b-a)^{q-1}} \quad a \le d \le b, \tag{7}$$

in which, $\Gamma(\cdot)$ is the gamma function, a, b, p and q are the parameters of the beta distribution, where they are assumed as $a = 0$, $b = 6$, $q = 8$, and p is given by:

$$p = q \cdot (0.007 \cdot \mu_D^3 - 0.0525 \cdot \mu_D^2 + 0.2875 \cdot \mu_D), \tag{8}$$

Thus, using Eqs. (6–8), the fragility curves to be used in the modelling of the damage due to the occurrence of a macroseismic intensity I can be completely defined as:

$$P(D > d \mid I) = 1 - P_{\beta \mid I}(d), \tag{9}$$

6.3 Strategic public buildings: schools, hospitals and security buildings

Data were extracted from the *Lavori Socialmente Utili* (LSU; Socially Useful Work) framework database (Cherubini et al. 1999) that was derived from the vulnerability surveys for the main health facilities (hospitals), schools, municipal offices and military structures, carried out in southern Italy. For the schools, individual positions and vulnerability data were also obtained from sheet forms that were collected during the 1996–2001 LSU project of the Civil Defence Protection. The LSU surveys were conducted using tools that have been extensively tested (e.g., the vulnerability sheet forms, levels I and II, of the GNDT), and also more experimentally with new instruments that were specifically designed according to individual projects. The results of these surveys have been included in publications issued by the Department of Civil Protection and managed by the GNDT (Cherubini et al. 1999).

There were 402 geocoded vulnerability sheets forms for schools in the study area, whereas there were 64 and 16 for security and health buildings, respectively. For these strategic public buildings, the vulnerability index was evaluated using the GNDT approach, which was based on an analysis proposed by Benedetti and Petrini (1984). According to this method, 11 parameters that are related to components and to qualitative features of the buildings were identified as crucial to assess how prone a building is to damage by ground shaking. Each parameter is given a score p_i that ranges from poor to good condition (D to A), while the overall vulnerability index, V_u, is given by:

$$V_u = \sum p_i w_i \tag{10}$$

where w_i is the weight that measures how important the parameter i is with respect to the other parameters. The scores and weights were determined through statistical analysis of the data collected after recent earthquakes. The final score can range from 0, when the present building code requirements are met, to 100, for very vulnerable structures (Table 5).

From Frassine and Giovinazzi (2004), it is possible to derive Eq. (11), which relates the above vulnerability index Vu used by GNDT method described above with the I_V proposed by Lagomarsino and Giovinazzi (2006) and adopted in this project for residential buildings in large areas:

$$I_V = 156.25 * V_u - 76.25 \tag{11}$$

Table 5 Numerical scale of the vulnerability index, V_u

i	Parameter	Condition score p_i				w_i
		A	B	C	D	
1	Resistance system organisation	0	0	20	45	0.261
2	Resistance system quality	0	5	25	45	0.065
3	Conventional resistance	0	5	25	45	0.392
4	Position of the building and foundations	0	5	25	45	0.196
5	Diaphragms	0	5	15	45	(*) var.
6	Plan configuration	0	5	25	45	0.131
7	Elevation configuration	0	5	25	45	(*) var.
8	Maximum distance between walls	0	5	25	45	0.065
9	Roof type	0	15	25	45	(*) var.
10	Non-structural elements	0	0	25	45	0.065
11	Preservation state	0	5	25	45	0.261

The weight of parameters 5, 7 and 9 vary in the range 0.131–0.261, depending on the percentage of rigid well-connected diaphragms, the presence of soft storey or pilotis, and the roof weight

(*) var. means variable

6.4 Physical infrastructure and systems

6.4.1 Road network

Within the dense network of roads running through the study area (including the Catania-Messina state road, which runs along the coast on the eastern flank of Mt. Etna), only the motorway bridges have been considered (for the A18 Messina to Catania motorway), as these are the most sensitive elements. On this road, there are 50 geocoded vulnerability forms of bridges with typological classifications. The following information is included in the data: street name, typology, year of construction, type of pillars, materials of pillars, bridge name, bridge length, and type of joints, among others. Their vulnerabilities were assigned according to this typological classification. Bridge damage was evaluated according to the damage classification proposed in the Portuguese '*Estudo do Risco Sísmico e de Tsunamis do Algarve*' (ERSTA) project (ERSTA 2008) and provided in Appendix (Table 9). For the analytical functions of the fragility curves for the bridges adopted in the present study, see Table 3.

6.4.2 Electricity power stations and local electricity transformers

For the electricity power network, an estimation of the typology of the facilities was performed through analysis of aerial photographs taken at each site. While it was possible to identify eight power stations (Table 6), no information was available about lower level facilities, such as small transformers. In this case, these were assumed to be of the 'aerial' type, and it was assumed also that there was at least one of these in each census area. This information on the electricity power stations was integrated into a field survey performed by the INGV local team that verified with analysis of aerial photographs of the area. The

Table 6 Locations of the electricity power stations

Latitude (°N)	Longitude (°E)	Municipality	Name
37.5325	15.0956	CATANIA	Cabina primaria 'Catania Nord'
37.7144	15.1602	MACCHIA	Cabina primaria 'Giarre'
37.6253	15.1137	LAVINAIO	Cabina primaria 'Viagrande 2'
37.6734	15.1450	LINERA	Cabina Primaria 'S. Venerina'
37.5804	15.0783	TREMESTIERI	Cabina Primaria 'S. Giovanni la Punta'
37.8169	15.2320	CALATABIANO	Cabina Enel Ferrovia
37.7272	15.1630	MONTEBELLO	Cabina primaria
37.5982	15.1642	ACIREALE	Cabina primaria ferrovia

electricity power stations in the area were inspected, and a photographic survey was carried out to collect information on the vulnerability of the installations (D'Amico and Tuvè 2013).

The performance of electricity power transformer substations after an earthquake is strongly influenced by the specific equipment design and installation practices. Some of the power system damage observed can be attributed to lack of, or inadequate, anchorage. In the present study, and according to the information from the visual inspection of the electrical equipment, we considered the equipment as not being anchored.

Electricity power station damage was evaluated according to the damage classification proposed in the 'Syner-G' project (Syner-G project—Deliverable D3.3 2010), and provided in Appendix (Table 10). For the analytical functions of the fragility curves for the electricity power transformers adopted in this study, see Table 3. According to the damage classification proposed in the ERSTA project (ERSTA 2008), damage to the small transformers was assumed to be binary, as 'no damage' or 'collapsed'.

6.4.3 Natural gas network

The infrastructure considered here was for natural gas pipelines and natural gas Pressure Reduction and Measurement Stations (PRMS). Unlike the electricity power network, an estimation of the typology of these facilities was not possible through an analysis of aerial photographs. The only information on the topology of the natural gas pipelines was taken from data collected by the Civil Protection of the Sicily Region (Provincia di Catania 2002). This information was integrated through a field survey performed by the INGV local team, which identified the natural gas PRMS of the area. A photographic survey was then carried out to collect information on the vulnerability of these installations (D'Amico and Tuvè 2013).

Eleven methane gas stations were identified, but no information was available about lower level facilities. For the natural gas pipeline network (more than 210 km of pipelines in the study area), the following information was available: the name of the network manager, the typology, and in few cases, the diameter of the pipes.

For the natural gas pipelines, in the absence of permanent ground displacement, the 'repair rate/km' was used for damage quantification, as proposed in the Syner-G project (Syner-G project—Deliverable D3.4 2010). From the same Syner-G project, for the natural gas PRMS, we used the discrete damage levels that are shown in Appendix (Table 11). For the analytical functions of the fragility curves for the natural gas pipelines and natural gas PRMS adopted in the present study, see Table 3.

6.4.4 Water and wastewater network

In the study area, 510 km of water pipelines and 250 km of wastewater pipes were identified. Also in this case, as for natural gas networks, an estimation of the typology of the facilities was not possible through an analysis of aerial photographs. The only information about the topology of these two networks was taken from data collected by the Civil Protection of the Sicily Region (Provincia di Catania 2002). The information available was the network company, the typology and the served municipalities. We note that the information about the wastewater pipeline networks only partially covers the study area. In the absence of permanent ground displacement, the 'repair rate/km' was used for damage quantification, as proposed in the HAZUS model (HAZUS MH MR4 2003). For the analytical function of the fragility curves for the water and wastewater networks adopted in this study, see Table 3.

6.4.5 Explosives storage and inflammable liquid tanks

For the explosives storage and inflammable liquid tanks, information was collected on the positions of depots and their typological classification, although without any information on the vulnerability of the stored materials. Additional information for the dangerous deposits was taken from data collected by the Civil Protection of the Sicily Region (Provincia di Catania 2002).

In the study area, four explosives storage and inflammable liquid tanks were identified. For these depots, the following information was available: name of the deposit, typology, municipality and location. The damage descriptors for explosives storage and inflammable liquid tanks used the descriptors proposed in the HAZUS model (HAZUS MH MR4 2003), and provided in Appendix (Table 12).

7 Damage to buildings, urban infrastructure and systems

As a brief summary, the physical structures exposed to earthquake impact that are considered in this case study are: residential buildings, primary and secondary schools, security buildings (i.e., police and fire stations, military structures), healthcare buildings, highway bridges, elements of the natural gas system (i.e., pipelines, gas pressure reduction measurement stations), electricity power stations (and local electricity transformers), water and wastewater pipelines, explosives and inflammable liquid tanks.

We present here in detail the estimates of damage for different vulnerability elements that has been carried out with the QuakeIST® software. The first level of analysis was obtained using the QuakeIST® software, which is based on obtaining intensity distributions analytically (e.g., Fig. 5, right, anisotropic model) and estimating the spatial distribution of the losses (e.g., building and lifeline damage) throughout the study area. The second level of analysis is intended for propagation effects using the DI rules.

7.1 Physical damage to buildings, urban infrastructure and systems

The following we illustrate the results expected from the simulation of an earthquake similar to the one occurred in 1914 along the S. Tecla fault, expressed in terms of damage in the study area. Figure 6a shows the mode of the damage grade distribution expected for
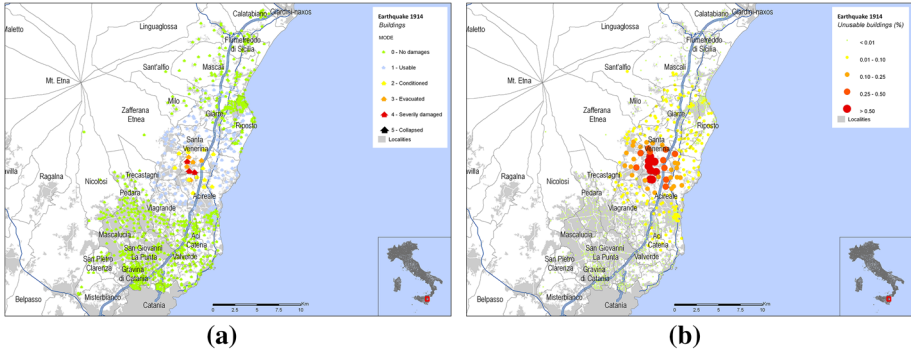
Fig. 6 Damage expected to residential buildings following an earthquake like the one occurred in 1914 along the S. Tecla fault. **a** Mode of damage grade distribution. **b** Percentage of unusable buildings

each census section, according to the classification of damage in the EMS scale. The results show three census sections with D4 (severely damaged), five census sections with D3 (evacuated) and 13 census sections with D2. In the rest of the study area damage would be negligible.

Figure 6b illustrates the percentages of unusable buildings among the residential buildings in the area. The buildings considered unusable include 40 % with damage of D3, with all of the other buildings with damage of D4 or D5. The results show three census sections with greater than 80 % unusable buildings, four census sections with 60–80 % unusable buildings, and four census sections with 40–60 % unusable buildings. In the rest of the study area, the unusable buildings are expected to be less than 40 %.

The expected school damage associated with the 1914 risk scenario is shown in Fig. 7a. As seen in the map, one school located in S. Venerina would suffer damage grade D4 (severely damaged), nine schools in Acireale would suffer damage grade D3 (evacuated), 10 schools in S. Venerina, Acireale and Aci S. Antonio would suffer damage grade D2 (conditioned); in all of the rest of the study area the schools would remain operational.

The expected damage to security buildings (i.e., police and fire stations, military structures) associated with this shaking scenario is shown in Fig. 7b. Only two security centres in S. Venerina would suffer damage grade D2 (conditioned), while all of the other security centres would remain operational.
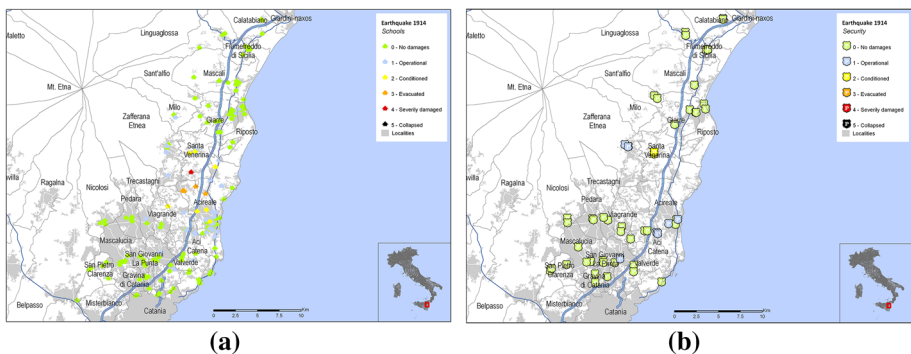

**Fig. 7** Damage to primary and secondary schools **a** and security buildings **b** in the study area

In terms of physical damage to hospitals and primary healthcare centres, Fig. 8a illustrates that in two healthcare buildings in Giarre, damage grade D2 (conditioned) would be expected, whereas in the rest of the study area, all of the healthcare centres would remain operational. However, the adverse impact on the healthcare system would cover a larger proportion of the hospitals and primary health centres due to propagation effects from other important lifelines, like the power and water systems, and due to problems of mobility. As far as bridges are concerned, Fig. 8b shows that all of the motorway bridges in the study area (i.e., 50 bridges along the Catania-Messina A18 highway) would remain operational.

For the physical damage to the natural gas systems, it is necessary to consider damage to natural gas pipelines and PRMS. Figure 9a, b shows these effects in two different maps. We see that only two sections of the natural gas pipeline, in S. Venerina and Acireale, would need to be repaired, and that through all of the study area, no damage would be expected to the PRMS.

Figure 10a illustrates the damage that would be expected to be inflicted on the electricity power stations. The results show that the power station in S. Venerina (Linera) would suffer extensive damage, but no damage would be expected to the other power stations.
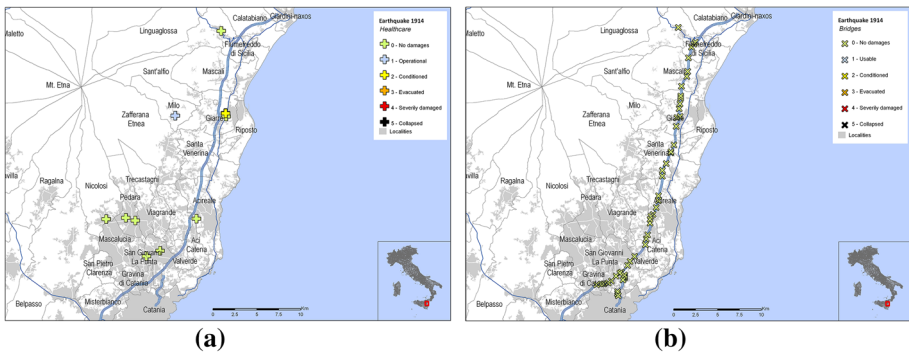
Fig. 8 Damage to healthcare buildings **a** and motorway bridges **b** in the study area
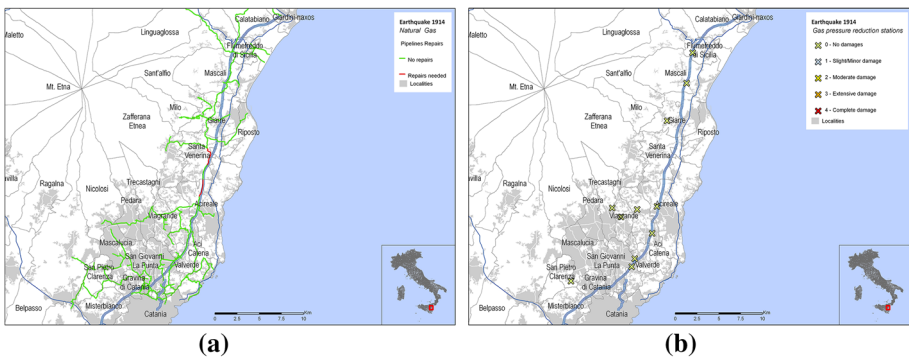
Fig. 9 Damage to the natural gas system in the study area. **a** Pipelines. **b** Pressure reduction and measurement stations
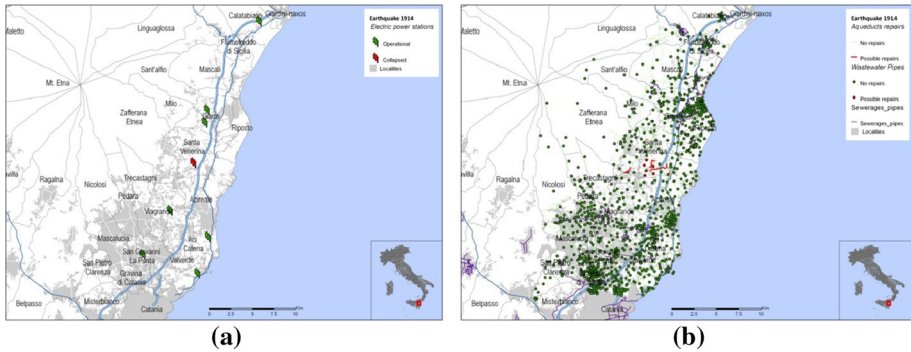
Fig. 10 Damage to the electricity power stations **a** and water and wastewater systems **b** in the study area

For physical damage to the water and wastewater systems, it is necessary to consider the damage to the two different pipeline networks separately. Figure 10b shows these effects with different symbols on the map. For the water distribution system, while a few sections of the network of S. Venerina and Zafferana Etnea would need to be repaired, no other repairs would be needed to the water pipelines. For the wastewater network, in S. Venerina, a few points of the pipeline would need to be repaired, but no significant damage would be expected in the rest of the area.

Finally, for the explosives and inflammable liquid tanks in the study area (Fig. 11a), one deposit in S. Venerina would be completely damaged, one in Acireale would show moderate damage, whereas in the rest of the study area there would be no damage to the explosives deposits.

7.2 Evaluation of the functional disruption (human needs)

After evaluation of the physical damage to the infrastructure due to the 1914 earthquake scenario (Io = IX-X EMS98), the DI was used to assess the phases required to evaluate the impact to services and components, and consequently for evaluation of the interruption of the functions (also described as 'human needs'). For the area of human needs identified as 'Environment' (Fig. 11b), the functional disruption was based on the water and sanitation
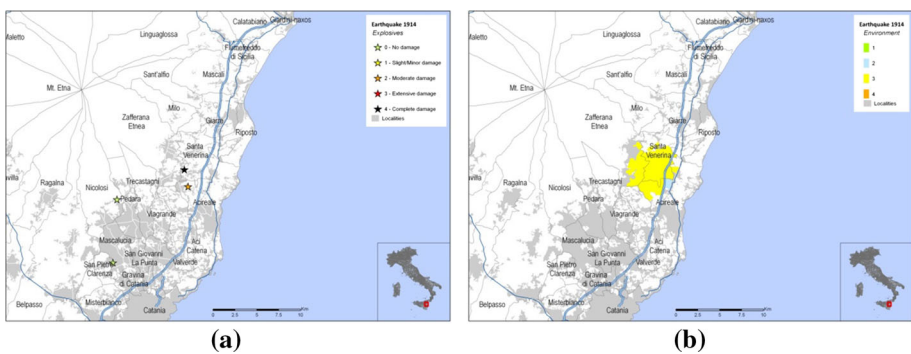
Fig. 11 **a** Damage to explosives and inflammable liquids tanks. **b** Estimated functional disruption (human needs): 'Environment'

supply services. The main impact level evaluated for the 'Environment' area was level 3. According to the definition of the DI, these estimated effects are sanitation problems with health impact, and building waste/debris problems. Contaminated drinking water (due to sewage contamination and to seawater contaminated with sewage) poses a serious health threat, with the risk of disease.

For the area of human needs identified as 'Food' (Fig. 12a), the functional disruption was based on the following services and dependencies: mobility and security. The main impact level evaluated for the 'Food' area was level 2. According to the definition of the DI, the estimated effects are disruption of normal conditions for food delivery, mainly due to mobility difficulties. The supply is provided by the Civil Protection and/or other institutions.
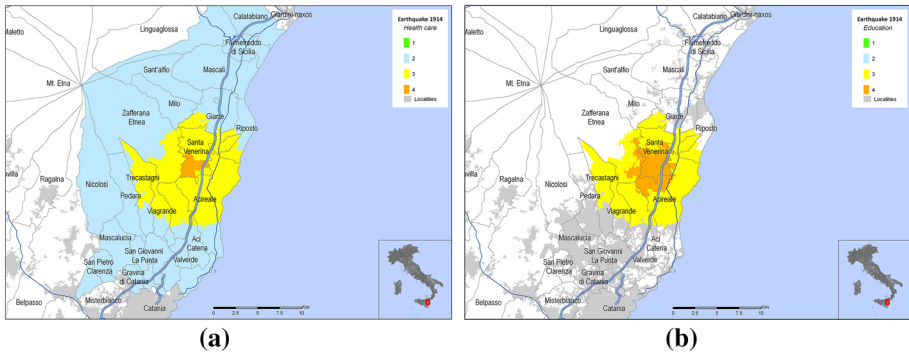
For the area of human needs identified as 'Housing' (Fig. 12b), the functional disruption was based on the following services and critical infrastructure dependencies: buildings, mobility, power supply, water supply and sanitation supply. The main impact level evaluated for the 'Housing' area was level 4. According to the definition of the DI, the estimated effects are for unusable residential buildings (>40 % for D3 and D4 + D5), and need for semi-permanent housing and long-term relocation. The displacement of residents from their houses significantly alters the traffic patterns, combined with changes in the locations of schools, businesses and shops.

For the area of human needs identified as 'Healthcare systems' (Fig. 13a), the functional disruption was based on the following services and critical infrastructure dependencies: healthcare facilities, security, mobility, power supply, water supply and sanitation supply. The main impact level evaluated for the 'Healthcare' area was level 3. According to the definition of the DI, the estimated effects are: provision of only the basic healthcare, and reduced capacity for surgery to minimise the risk of post-operative infection; health personnel in need of better coordination to provide medical services and deliver assistance; problems of distribution and availability of essential medicines; forced evacuation of patients at damaged hospitals and healthcare centres to temporary and/or provisional medical care centres.
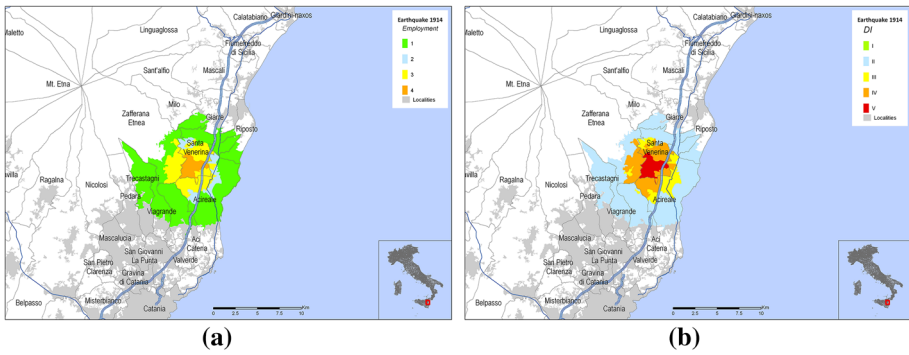
For the area of human needs identified as 'Education' (Fig. 13b), the functional disruption was based on the following services and critical infrastructure dependencies: educational facilities, mobility, power supply, water supply and sanitation supply. The main impact level evaluated for the 'Education area' was level 3. According to the definition of the DI, the estimated effects are: difficult access to education; educational facilities with severe damage or collapse, or restricted access due to debris; teachers not
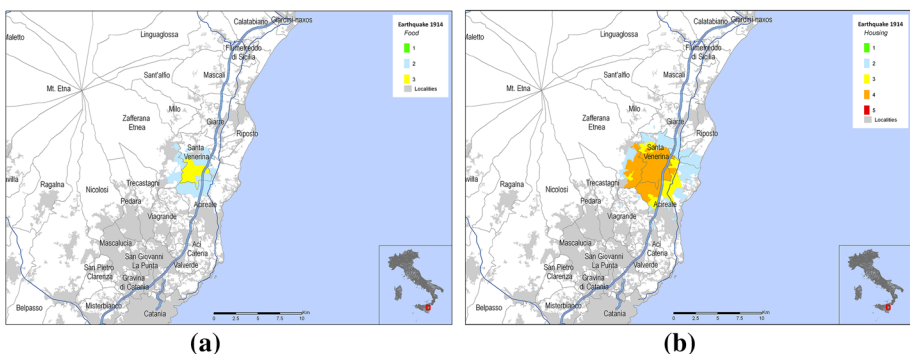
Fig. 12 Estimated functional disruption (human needs): **a** Food. **b** Housing

Fig. 13 Estimated functional disruption (human needs): **a** healthcare systems. **b** Education

Fig. 14 **a** Estimated functional disruption (human needs): 'Employment'. **b** Estimated Disruption Index for the study area

able to gain access, and materials destroyed; need for temporary relocation or sharing of the school site with another school, until completion of rehabilitation works.

For the area of human needs identified as 'Employment' (Fig. 14a), the functional disruption was based on the following services and critical infrastructure dependencies: buildings, mobility, power supply, water supply and sanitation supply. The main impact level evaluated for the 'Employment' area was level 3. According to the definition of the DI, the estimated effects are: interruption of most economic activity; sales/production decrease.

7.3 Disruption Index assessment for the Mt. Etna area

The final level of analysis of the DI assessment procedure was based on the propagation effects of the earthquake impact that are produced by functional disruption (i.e., of human needs), as established using the DI rules (see Ferreira et al. 2015). The results for the DI procedures are shown in Fig. 14b, as applied for the evaluation of physical damage to the infrastructure due to the 1914 scenario earthquake estimated for the study area.

The quantification of the estimated effects in the study area is presented in Table 7, with the qualitative descriptors of the DI grades also provided.

Table 7 Quantification of the estimated Disruption Index effects

Disruption Index scale	Quantification
II	77 km^2 (70 % of the study area); 43,849 inhabitants affected (80 % of the population)
	The region affected by the disaster results in some homeless people (about 5 %) due to damage to buildings, which affects the habitability of a given geographical area. Some of the people experience problems of access to water, electricity and/or gas. Some cases required temporary relocation
III	9 km^2 (8 % of the study area); 3601 inhabitants affected (7 % of the population)
	Part of the population permanently lose their property and need permanent relocation, which means strong disturbance to their everyday life. This level represents significant dysfunction in terms of equipment, critical infrastructure, and loss of some assets, and certain disorders involving the conduct of professional activities, for some time. The most affected areas show significant problems in mobility due to debris or damage to the road network. There is the start of significant problems in providing food and water, which must be ensured by the Civil Protection
IV	18 km^2 (17 % of the study area); 4865 inhabitants affected (9 % of the population)
	Start of paralysis of the main buildings, housing, administrative and political systems. The region affected by the disaster suffers moderate damage and a percentage of total collapse of buildings, as well as victims and injuries. There is a considerable number of homeless, because their houses have been damaged, and although they have not collapsed, this is enough to lose their function for housing. Normal daily activities are disrupted; school activities are suspended; economic activities are at a standstill
V	5 km^2 (5 % of the study area); 2308 inhabitants affected (4 % of the population)
	From serious disruption at both the physical and functional levels, to paralysis of the entire system: buildings, population, infrastructure, health, mobility, administrative and political structures, among others. Lack of conditions for the functions and activities of daily life. High cost for the recovery

This is the final result of the application of the Disruption Index, which comprises a total area of 509 km^2 (total area of Etna region), with a total population of 324,481 inhabitants, and where the target area is 109 km^2 (21 % of the total area) and the target population is 54,623 inhabitants (17 % of the total population).

8 Assessment of the importance of the components of the urban system

In light of the estimated effects illustrated in the previous section and shown in Fig. 14b, it could be asked, e.g., which prevention strategies need to be given priority to reduce levels IV and V of disruption in such a large part of the affected area, to level II. Level II appears to be an 'acceptable' level of disruption. Carrying out this optimal reduction might come at appreciable cost. Only a cost-benefit analysis can be used to determine the practical implementation of these priority measures.

To answer the above question, we need first to understand to what extent the different human needs dimensions contribute to the disruption, which can be achieved through an analysis of the modelling of the propagation of the severity. Let us consider, e.g., level V of the DI. From the definition of the DI, we know that this might arise from level V disruption of the 'Housing' dimension, from level III disruption of the 'Food' dimension, or from level IV disruption of the 'Environment' dimension (Ferreira et al. 2014). In their turn, level V disruption of the 'Housing' dimension derives from level V disruption of the building stock, level III disruption of the 'Food' dimension derives from level IV

disruption of the mobility and/or security functions, and so on. From the definition of the DI, we also know that to have a DI of level II, the 'Employment' dimension must have a disruption level ≤II and the 'Healthcare' and 'Education' dimensions must have disruption levels ≤III. Then, to have a DI of level III, the 'Housing' dimension must be <IV, and so on.

Following the network of dependencies in the bottom-up sequence due to the physical assets exposed to risk, we can understand their contributions to the disruption. We see, e.g., that to maintain a disruption level of II for the 'Employment' dimension, we must have a disruption level of the electricity power stations ≤II, and that we cannot have a disruption of the school buildings >III if we want a level of disruption ≤III for the 'Education' dimension. On the other hand, e.g., we see that if the amount of debris corresponds to level III disruption, mobility reaches level IV, the 'Food' dimension reaches level IV, and the DI will reach its maximum of V.

An understanding of the extent to which the physical assets contribute to the overall disruption of a system will suggest the potential prevention strategies, although it is clear that there are many degrees of freedom that any prevention strategy can have, given the complexity of the system under consideration here. Indeed, in the study area there are >300 typological classes of buildings, the road network includes 50 vulnerability forms of bridges with typological classifications, there are >400 vulnerability sheet forms for the schools, 16 vulnerability forms for the healthcare facilities, and >60 vulnerability forms for the security buildings, plus a certain number of electric and gas stations, and >300 water pipeline branches, and so on.

Combining the risk evaluation and the consequent urban dysfunction with the need to find alternatives to reduce or constrain the risk, we explored the risk-analysis field, which is greatly interrelated with our aim. To accomplish this goal, 'risk importance measures' are defined to evaluate the importance of a feature in further reduction of the risk, and its importance in the maintenance of the present risk level. One of these risk importance measures is the so-called 'Risk Reduction Worth' (RRW), which is useful for exploring the potential of the components to reduce the global level of disruption. Another of these risk importance measures is the 'Risk Achievement Worth' (RAW), which is useful for exploring the potential of the components to worsen the global level of disruption. To be more precise, the RRW compares a reference risk with one that would be achieved if the component of interest decreased its level of dysfunction, whereas the RAW compares a reference risk with one that would be achieved if the component of interest increased its level of dysfunction.

Another useful measure is the so-called 'Birbaum Index' (Van der Borst and Schoonakker 2001), which compares the level of risk derived from changes in the state of dysfunction of the components of the system without considering a reference level of risk. The Birbaum Index is particularly suitable when the physical damage suffered by the exposed elements is obtained by simulation of different damage scenarios, and is not derived from inspection after the event.

In the following, we provide an example of the use of the RRW to evaluate the potential of the residential building vulnerability to reduce the disruption in the Mt. Etna area. More specifically, we consider level III disruption and explore how the area affected by this level of disruption can change by reducing the vulnerability of all of the residential buildings by 5, 10 and 30 %. The RRW is defined here in terms of the ratio between the original area affected by the level III disruption and the area that would suffer level III disruption if the residential buildings vulnerability was reduced. The results are given in Table 8. Here, the

Table 8 Risk Reduction Worth values obtained by reducing the building stock vulnerability

Disruption Index scale	Vulnerability of the building stock	Area (km^2)	Area (%)	Inh. (n)	Inh. (%)	Risk Reduction Worth
II	Original	77	70	43,849	80	–
III	Original	**9**	8	3601	7	–
IV	Original	18	17	4865	9	–
V	Original	5	5	2308	4	–
II	5 % decrease	80	73	45,852	84	0.96
III	5 % decrease	**6**	6	1598	3	**1.50**
IV	5 % decrease	18	17	4865	9	1.0
V	5 % decrease	5	5	2308	4	1.0
II	10 % decrease	82	75	45,977	84	0.94
III	10 % decrease	**4**	3	1473	3	**2.25**
IV	10 % decrease	18	17	4865	9	1.00
V	10 % decrease	5	5	2308	4	1.00
II	30 % decrease	83	76	45,985	84	0.93
III	30 % decrease	**3**	2	1465	3	**3.00**
IV	30 % decrease	18	17	4865	9	1.00
V	30 % decrease	5	5	2308	4	1.00

Bold values indicate the level of disruption (III) used as reference in the example

Inh. inhabitants

reductions in vulnerability taken into account (i.e., 5, 10, 30 %) correspond to RRW values of 1.50, 2.25 and 3.00, respectively. Figure 15 shows these changes in the affected areas.

This RRW ratio is always ≥1.00, and defines the maximum risk reduction (in our case, the impact reduction, or DI) that is possible following an improvement in the building stock.

Different definitions of the RRW can obviously be taken into account. For example, the RRW could be defined in terms of the ratio between inhabitants of the affected area, in which case we would obtain values of the RRW that are much more stable (i.e., 2.25, 2.44 and 2.46, for 5, 10 and 30 % reductions in vulnerability, respectively). Generally speaking, the choice of how to define the risk importance measures should depend on the area under study and the results that are required by application of such prevention strategies. Ferreira et al. (2015) present the formal definitions of the RRW and RAW, and develop a more refined algorithm.

9 Conclusive remarks and future developments

The present work explains in detail how to evaluate and measure the impact of an earthquake in an urban area that is subjected to a high level of seismicity, like Mt. Etna. This has been achieved by applying knowledge and recent research in the fields of geological earthquake sources, hazard analysis, data collection of different elements at risk and their vulnerability, scenario simulations, and urban disruption.

The interest for a study like this is not only to obtain an objective, numerical measure of damage, but also to highlight the importance of taking a holistic view of this problem. This
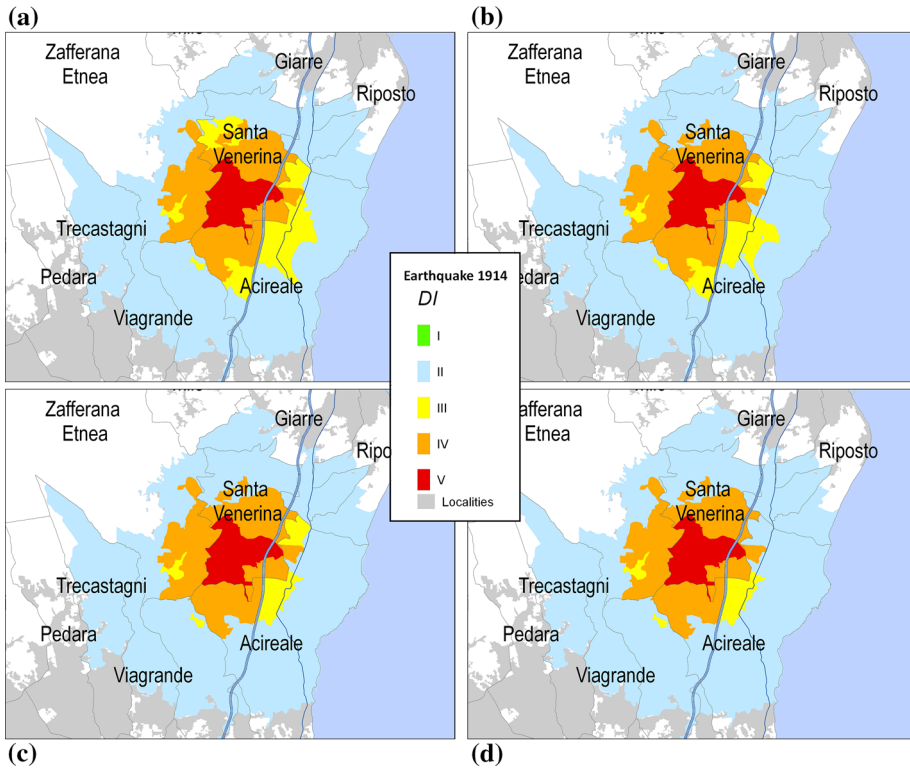
Fig. 15 The DI maps that are obtained by decreasing the building stock vulnerability, according to the original value **a**, and to decreases in the building stock vulnerability of 5 % **b**, 10 % **c** and 30 % **d**

study illustrates the need to consider all of the dimensions of the urban system, to identify their interactions and the consequences of these interactions in a simple and understandable way. In this study, starting from different testing analyses, we have selected only a specific earthquake scenario (the one similar to the 1914 earthquake) to highlight the implemented procedure. With this output, it is possible to use the importance measures of the RRW although we would advise careful consideration towards any reduction of the vulnerability elements, which needs to be done in a conscious manner, while also taking into account the costs and benefits of such interventions.

In the example considered here, we have empirically reduced the vulnerability of all building stock considered without any precise physical intervention regarding retrofitting. On the other hand, we have not considered the cost of these actions, which should indeed be considered in a real application.

In the illustration presented (Fig. 15), it is interesting to note that the results are controlled by the human need of 'Housing', and that only the DI grade of III shows any appreciable change for the impact area.

Future studies in this area to prioritise the type of interventions that can be followed to reduce the risk should include an analysis of the most critical typologies, and not reduce the vulnerability in a simple way. Reductions in the DI from IV or V will require large interventions, with the corresponding necessary investment. Thus, only a cost-benefit analysis can provide the constrain information regarding the 'best' management policies.

Appendix

See Tables 9, 10, 11 and 12.

Table 9 Classification of the damage to bridges

Grade	Damage level
1	Slight damage
	Small cracks and peeling at joints; cracking of 'shear keys' at joints; small concrete peeling at flanges and pillars (damage that needs 'cosmetic' repair); small cracks in road surface
2	Moderate damage
	Pillars with moderate cracking and peeling of concrete, while maintaining a solid look; movement of moderate joints (<5 cm); extensive cracking and spalling of shear keys, some connections with cracked shear keys or bent bolts; keeper bar failure without unseating; moderate settlement of near embankment
3	High damage
	Greatly degraded pillars, although without collapse (shear failure), but structurally unsafe; important movement in residual joints; significant settling of the landfill approach; vertical settling of joints; differential settling of joints; rupture of 'shear keys' at joints
4	Collapse
	Pillar collapse or loss of ability to provide support, which could jeopardise the safety of the road surface; rotation by rupture of the foundation structure

Table 10 Classification of damage to electricity power stations

Grade	Damage level
1	Slight/minor damage
	Failure of 5 % of the disconnect switches (i.e., misalignment), or failure of 5 % of the circuit breakers (i.e., circuit breaker phase sliding off its pad, circuit breaker tipping over, or interrupter-head falling to the ground), or the building being in a minor damaged state. Reduced power flow. Operational without repair
2	Moderate damage
	Failure of 40 % of the disconnect switches (e.g., misalignment), or 40 % of the circuit breakers (e.g., circuit breaker phase sliding off its pad, circuit breaker tipping over, or interrupter-head falling to the ground), or failure of 40 % of the current transformers (e.g., oil leaking from transformers, porcelain cracked), or the building being in a moderately damaged state. Reduced power flow. Operational without repair
3	Extensive damage
	Failure of 70 % of the disconnect switches (e.g., misalignment), 70 % of the circuit breakers, 70 % of the current transformers (e.g., oil leaking from transformers, porcelain cracked), or failure of 70 % of the transformers (e.g., leakage of transformer radiators), or the building being in an extensively damaged state. No power available. Operational after repairs
4	Complete damage
	Failure of all of the disconnect switches, all of the circuit breakers, all of the transformers, or all of the current transformers, or the building being in a completely damaged state. No power available. Not repairable

Table 11 Classification of damage to natural gas pressure reduction and measurement stations

Grade	Damage level
1	Slight/minor damage Slight damage to buildings or full loss of commercial power and back-up power for a few (<3) days
2	Moderate damage Considerable damage to mechanical and electrical equipment, or considerable damage to buildings, or loss of electrical power and of back-up for 7 days
3	Extensive damage Buildings extensively damaged, or pumps badly damaged; beyond repair
4	Complete damage Building collapse

Table 12 Classification of damage to explosives storage and inflammable liquid tanks

Grade	Damage level
1	Slight/minor damage Damage to roof, minor loss of contents, minor damage to piping, but no 'elephant-foot' buckling
2	Moderate damage 'Elephant-foot' buckling, with minor loss of contents
3	Extensive damage 'Elephant-foot' buckling, with major loss of contents; severe damage
4	Complete damage Total failure; tank collapse

References

Agostinelli C, Rotondi R (2015) Analysis of macroseismic fields using statistical data depth functions. Considerations leading to attenuation probabilistic modelling. Bull Earthq Eng. doi:10.1007/s10518-015-9778-2

Alparone S, Andronico D, Giammanco S, Lodato L (2004) A multidisciplinary approach to detect active pathways for magma migration and eruption at Mt. Etna (Sicily, Italy) before the 2001 and 2002–03 eruptions. J Volcanol Geoth Res 136(1–2):121–140

Azzaro R (2004) Seismicity and active tectonics in the Etna region: constraints for a seismotectonic model. In: Bonaccorso A, Calvari S, Coltelli M, Del Negro C, Falsaperla S (eds) Mt. Etna: volcano laboratory. American Geophysical Union, Geophysical monograph, 143, Washington, DC, pp 205–220

Azzaro R, D'Amico S, Tuvè T (2011) Estimating the magnitude of historical earthquakes from macroseismic intensity data: new relationships for the volcanic region of Mount Etna (Italy). Seismol Res Lett 82(4):533–544

Azzaro R, D'Amico S, Peruzza L, Tuvè T (2013a) Probabilistic seismic hazard at Mt. Etna (Italy): the contribution of local fault activity in mid-term assessment. J Volcanol Geoth Res 251:158–169

Azzaro R, D'Amico S, Rotondi R, Tuvè T, Zonno G (2013b) Forecasting seismic scenarios on Etna volcano (Italy) through probabilistic intensity attenuation models: a Bayesian approach. J Volcanol Geoth Res 251:149–157

Azzaro R, D'Amico S, Tuvè T (2015) Seismic hazard assessment in the volcanic region of Mt. Etna (Italy): a probabilistic approach by macroseismic data applied to local volcano-tectonic seismicity. Bull Earthq Eng (under review for this issue)

Behncke B, Neri M, Nagay A (2005) Lava flow hazard at Mount Etna (Italy): new data from a GIS-based study. In Manga M, Ventura G (eds) Kinematics and dynamics of lava flows. Geological Society of America Special Paper 396, pp 189–208. doi:10.1130/2005.2396(13)

Benedetti D, Petrini V (1984) On seismic vulnerability of masonry buildings: proposal of an evaluation procedure. L'industria delle Costruzioni 18:66–78

Bernardini A, Giovinazzi S, Lagomarsino S, Parodi S (2007) The vulnerability assessment of current buildings by a macroseismic approach derived from the EMS-98 scale. In: Proceedings of the 3th Congreso Nacional de Ingenieria Sismica, Asociación Española de Ingeniería Sísmica, Girona

Branca S, Carbone D, Greco F (2003) Intrusive mechanism of the 2002 NE-Rift eruption at Mt. Etna (Italy) inferred through continuous microgravity data and volcanological evidences. Geophys Res Lett 30(20):2077. doi:10.1029/2003GL018250

Cherubini A, Corazza L, Di Pasquale G, Dolce M, Martinelli A, Petrini V (1999) Risultati del progetto LSU-1. In: Censimento di vulnerabilità degli edifici pubblici, strategici e speciali nelle regioni Abruzzo, Basilicata, Calabria, Campania, Molise, Puglia e Sicilia. Graphic Press s.r.l., L'Aquila, Italy

CMTE Working Group (2014) Catalogo Macrosismico dei Terremoti Etnei, 1832-2013. INGV, Catania. http://www.ct.ingv.it/macro/etna/html_index.php

Crowley H, Colombi M, Borzi B, Faravelli M, Onida M, Lopez M, Polli D, Meroni F, Pinho R (2009) A comparison of seismic risk maps for Italy. Bull Earthq Eng 7(1):149–180

D'Amico S, Tuvè T (2013) INGV data survey for UPStrat-MAFA project, internal report

D'Amico S, Meroni F, Sousa ML, Zonno G (2015) Building vulnerability and seismic risk analysis in the urban area of Mt. Etna volcano (Italy). Bull Earthq Eng (under review for this issue)

Del Negro C, Cappello A, Neri M, Bilotta G, Herault A, Ganci G (2013) Lava flow hazards at Mount Etna: constraints imposed by eruptive history and numerical simulations. Sci Rep 3:3493. doi:10.1038/srep03493

ERSTA (2008) Project "ERSTA—Estudo do Risco Sísmico e de Tsunamis do Algarve"

Ferreira MA (2012) Risco sísmico em sistemas urbanos. Ph.D. Thesis, Instituto Superior Técnico, Universidade Técnica de Lisboa. (in portuguese)

Ferreira MA, Mota de Sá F, Oliveira CS (2014) Disruption Index, DI: an approach for assessing seismic risk in urban systems (theoretical aspects). Bull Earthq Eng 12(4):1431–1458

Ferreira MA, Mota de Sá F, Oliveira CS (2015) The Disruption Index (DI) as a tool to measure disaster mitigation strategies. Bull Earthq Eng (under review for this issue)

Frassine L, Giovinazzi S (2004) Basi di dati a confronto nell'analisi di vulnerabilità sismica dell'edilizia residenziale: un'applicazione per la città di Catania. In: Proceedings of the XI Congresso Nazionale "L'ingegneria Sismica in Italia", Genova, Italy, CD-Rom

Giovinazzi S, Lagomarsino S (2001) Una metodologia per l'analisi di vulnerabilità sismica del costruito. In: Proceedings of the X Congresso Nazionale "L'ingegneria Sismica in Italia", Potenza-Matera, CD-Rom

Grimaz S (2014) Can earthquakes trigger serious industrial accidents in Italy? Some considerations following the experiences of 2009 L'Aquila (Italy) and 2012 Emilia (Italy) earthquakes. Bollettino di Geofisica Teorica e Applicata 55(1):227–237

Grünthal G (ed) (1998) European Macroseismic Scale. Conseil de ĺEurope, Cahiers du Centre Européen de Géodynamique et de Séismologie, Vol. 15. Luxemburg

HAZUS MH MR4 (2003) "Technical Manual", Federal Emergency Management Agency. https://www.fema.gov/hazus

ISTAT (1991) 13° censimento generale della popolazione, 1991. Dati sulle caratteristiche strutturale della popolazione e delle abitazioni, Roma

Lagomarsino S, Giovinazzi S (2006) Macroseismic and mechanical models for the vulnerability and damage assessment of current buildings. Bull Earthq Eng 4:415–443

Locati M, Camassi R, Stucchi M (a cura di) (2011). DBMI11, la versione 2011 del Database Macrosismico Italiano. Milano, Bologna. http://emidius.mi.ingv.it/DBMI11

Meroni F, Petrini V, Zonno G (1999) Valutazione della vulnerabilità di edifici su aree estese tramite dati ISTAT, Atti 9° Convegno Nazionale ANIDIS: L'ingegneria Sismica in Italia, Torino (CD-ROM)

Meroni F, Petrini V, Zonno G (2000) Distribuzione nazionale della vulnerabilità media comunale. In: Bernardini A (ed) La vulnerabilità degli edifici. CNR-GNDT, Roma, pp 105–131

MPS Working Group (2004) Redazione della mappa di pericolosità sismica prevista dall'Ordinanza PCM 3274 del 20 marzo 2003. Final report for the Civil Protection Department, INGV, Milan-Rome

Mota de Sá F, Ferreira MA, Oliveira CS (2015) QuakeIST ®: earthquake scenario simulator using interdependencies. Bull Earthq Eng (under review for this issue)

Oliveira CS, Ferreira MA, Mota de Sá F (2012) The concept of a disruption index: application to the overall impact of the July 9, 1998 Faial earthquake (Azores islands). Bull Earthq Eng 10:7–25

Oliveira CS, Ferreira MA, Mota de Sá F (2014) Earthquake risk reduction: from scenario simulators including systemic interdependency to impact indicators. Perspect Eur Earthq Eng Seismol Geotech Geol Earthq Eng 34(9):309–330. doi:10.1007/978-3-319-07118-3_9

Platania G (1915) Sul periodo sismico del Maggio 1914 nella regione orientale dell'Etna. Mem. Cl. Sci. R. Acc. Zelanti. 7(3):48

Provincia di Catania (2002) Programma Provinciale di Protezione Civile—Tavole Tematiche. Provincia Regionale di Catania, Italy, CD-ROM

Rotondi R, Zonno G (2004) Bayesian analysis of a probability distribution for local intensity attenuation. Ann Geophys 47(5):1521–1540

Rotondi R, Zonno G (2010) Guidelines to use the software PROSCEN. Open archives earth-prints Repository, INGV, Reports. http://hdl.handle.net/2122/6726

Rotondi R, Brambilla C, Varini E, Sigbjörnsson R (2012) Probabilistic analysis of macroseismic fields: Iceland case study. In: 15th World Conference on Earthquake Engineering (15WCEE), Lisbon

Rotondi R, Varini E, Brambilla C (2015) Probabilistic modelling of macroseismic attenuation and forecast of damage scenarios. Bull Earthq Eng. doi:10.1007/s10518-015-9781-7

Rovida A, Camassi R, Gasperini P, Stucchi M (eds) (2011) CPTI11, the 2011 version of the Parametric Catalogue of Italian Earthquakes. Milano, Bologna. http://emidius.mi.ingv.it/CPTI. doi:10.6092/INGV.IT-CPTI11

Sabatini V (1913) Note sul terremoto di Linera dell'8 maggio 1914. Boll R Comit Geol It, s. V, XLIV(3):245–293

Sabatini V (1915) Considerazioni sismologiche a proposito del terremoto di Linera dell'8 maggio 1914. Boll. R. Comit. Geol. It XLV(3–4):197–222

Scollo S, Prestifilippo M, Spata G, D'Agostino M, Coltelli M (2009) Monitoring and forecasting Etna volcanic plumes. Nat Hazards Earth Syst Sci 9:1573–1585. doi:10.5194/nhess-9-1573-2009

Scollo S, Coltelli M, Bonadonna C, Del Carlo P (2013) Tephra hazard assessment at Mt. Etna (Italy). Nat Hazards Earth Syst Sci 13:3221–3233. doi:10.5194/nhess-13-3221-2013

Sicali S, Barbano MS, D'Amico S, Azzaro R (2014) Characterization of seismicity at Mt. Etna volcano (Italy) by inter-event time distribution. J Volcanol Geotherm Res 270:1–9

Syner-G project—Deliverable D3.3 (2010) Fragility functions for electric power system elements. http://www.vce.at/SYNER-G/

Syner-G project—Deliverable D3.4 (2010) Fragility functions for gas and oil system networks. http://www.vce.at/SYNER-G/

UPStrat-MAFA (2012–2013) Urban disaster prevention strategies using MAcroseismic Fields and FAult Sources (UPStrat-MAFA—EU Project Num. 23031/2011/613486/SUB/A5), DG ECHO Unit A5. Project Web page http://upstrat-mafa.ov.ingv.it/UPStrat/

Van der Borst M, Schoonakker H (2001) An overview of PSA importance measures. Reliab Eng Saf Syst 72:241–245

Zonno G, Rotondi R, Brambilla C (2009) Mining macroseismic fields to estimate the probability distribution of the intensity at site. BSSA 98(5):2876–2892. doi:10.1785/0120090042